Influence of doping on the Hall coefficient in $Sr_{14-x}Ca_xCu_{24}O_{41}$

E. Tafra,[1,][*] B. Korin-Hamzić,[2] M. Basletić,[1] A. Hamzić,[1] M. Dressel,[3] and J. Akimitsu[4]

[1]*Department of Physics, Faculty of Science, University of Zagreb, P.O. Box 331, HR-10002 Zagreb, Croatia*

[2]*Institute of Physics, P.O. Box 304, HR-10001 Zagreb, Croatia*

[3]*1. Physikalisches Institut, Universität Stuttgart, Pfaffenwaldring 57, D-70550 Stuttgart, Germany*

[4]*Department of Physics and Mathematics, Aoyama-Gakuin University, Sagamihara, Kanagawa 229-8558, Japan*

We present Hall-effect measurements of two-leg ladder compounds $Sr_{14-x}Ca_xCu_{24}O_{41}$ ($0 \leq x \leq 11.5$) with the aim to determine the number of carriers participating in dc transport. Distribution of holes between the ladder and chain subsystems is one of the crucial questions important for understanding the physics of these compounds. Our Hall-effect and resistivity measurements show typical semiconducting behavior for $x < 11.5$. However, for $x = 11.5$, the results are completely different, and the Hall coefficient and resistivity behavior are qualitatively similar to that of high-temperature copper-oxide superconductors. We have determined the effective number of carriers at room temperature and compared it to the number of holes in the ladders obtained by other experimental techniques. We propose that going from $x = 0$ to $x = 11.5$ less than 1 hole per f.u. is added to the ladders and is responsible for a pronounced change in resistivity with Ca doping.

I. INTRODUCTION

$Sr_{14-x}Ca_xCu_{24}O_{41}$ compounds are a part of the larger family $A_{14}Cu_{24}O_{41}$ ($A = Sr, Ca, La, Y, \ldots$) which are considered as quasi-one-dimensional (Q-1D) copper oxides due to their pronounced anisotropy. They have been investigated intensively during the last years because of their fascinating physical properties,[1,2] their close relation to cuprate superconductors,[3,4] and especially after the superconductivity was achieved under high pressure in a material heavily doped with Ca.[5]

The incommensurate crystal structures of these compounds consist of planes of quasi-one-dimensional CuO_2 chains stacked alternately with planes of two-leg Cu_2O_3 ladders.[6,7] The orientation of these chains and ladders defines the crystallographical **c** axis and are alternately stacked along the **b** axis separated by layers of Sr(Ca). Chain and ladder spin subsystems in $Sr_{14}Cu_{24}O_{41}$ interact weakly along the **a** axis. Consequently, the resistivity shows remarkable anisotropy, indicative of a quasi-one-dimensional electronic state.[8] Materials with different Sr/Ca composition are isostructural with only minor modifications of the bond lengths and angles.[9] All cuprate superconductors found up to now contain square CuO_2 planes, whereas $Sr_{14-x}Ca_xCu_{24}O_{41}$ is the only known superconducting copper oxide without a square lattice. An important feature of the superconductivity in $Sr_{14-x}Ca_xCu_{24}O_{41}$ is that it occurs by carrier doping in the low-dimensional antiferromagnetic spin system. This feature is common to the CuO_2 plane. Therefore, the evolution of the electronic structure upon hole doping is one of the key issues for understanding superconductivity.

$Sr_{14-x}Ca_xCu_{24}O_{41}$ is intrinsically hole doped due to stoichiometric reasons. In order for the formula unit to remain electrically neutral, the average copper valency must be +2.25 instead of +2. Thus, there is one hole per four Cu ions, or 6 per f.u. There are 4 f.u. per approximate superstructure cell, implying a hole density of $\sim 6 \times 10^{21}$ cm^{-3}. The often accepted doped hole density refers to one hole for every 14

Cu's in the ladder and five holes for every 10 Cu's in the chain (that are localized).

The Madelung potential calculations[10] have shown that for the $x = 0$ compound holes are staying essentially in the chains where their localization leads to an insulating behavior. Upon Ca substitution, which does not change the total hole count, holes are transferred from the chains to the ladders and the longitudinal conductivity (along the **c** axis) increases, leading to Q-1D metallic properties. This hole transfer can be caused by the reduction of the distance between chains and (Sr,Ca) layers, which results in an enhancement of the electrostatic potentials in the chains. The redistribution of the holes among chains and ladders (depending on the Ca content) is one of the most important factors which controls the physical properties (in particular superconductivity) of these spin ladders. However, experimentally, the precise amount of hole transfer is still under discussion, since different experimental techniques have provided contradictory results.

From the optical data, Osafune *et al.*[11] concluded that there is 1 hole per f.u. in the ladders for $x = 0$, and 2.8 for $x = 11$. Polarization-dependent near-edge x-ray-absorption fine structure (NEXAFS), as the technique which can probe the hole distribution between chains and ladders most directly, shows a much smaller hole transfer from the chains into the ladders induced by Ca substitution.[12] The results predict that 0.8 holes per f.u. are found in the ladders for $x = 0$ and 1.1 for the $x = 12$ compound. Also, Gotoh *et al.*[13] performed an x-ray diffraction study on $Sr_{14}Cu_{24}O_{41}$ crystals. The bond-valence sum calculation based on their data has indicated that only 0.5 holes per f.u. reside in the ladders for the $x = 0$ compound. Nuclear magnetic resonance (NMR) and nuclear quadrupole resonance (NQR) spectroscopy measurements were also performed on these compounds with different results.[14,15] Recently Piskunov *et al.*[16] reported results of a ^{63}Cu and ^{17}O study on $Sr_{14-x}Ca_xCu_{24}O_{41}$ for $x = 0$ and $x = 12$. They have found that the change in hole number is $n(x=12) - n(x=0) \approx 0.42$ holes per f.u. in the ladder, which is

in good agreement with NEXAFS results. They also reported that the hole distribution changes with temperature and pressure, concluding that the decrease in temperature reduces the hole number in the ladders by transferring them partly back to the chains, while pressure seems to induce an additional transfer of holes to the ladders. More recently, the distribution of holes in $Sr_{14-x}Ca_xCu_{24}O_{41}$ was revisited with semi-empirical reanalysis of the x-ray absorption.[17] This interpretation of the x-ray absorption spectroscopy (XAS) data lead to much larger ladder hole densities than previously suggested; i.e., it was concluded that there are 2.8 holes per f.u. in the ladders for $x=0$, and 4.4 for $x=11$.

The aim of this paper is to contribute to the undoubtedly still open question about the amount of holes that participate in the dc transport in $Sr_{14-x}Ca_xCu_{24}O_{41}$ for $0 \leq x \leq 11.5$, by studying the temperature dependence of the Hall coefficient—the long missing basic experiment. In our work, we emphasize the temperature region around room temperature where the obtained estimate for the effective number of carriers could be compared with the results obtained by different experimental methods.

II. EXPERIMENT

The $Sr_{14-x}Ca_xCu_{24}O_{41}$ ($0 \leq x \leq 11.5$) samples used in the present work were single crystals, made from calcined sintered polycrystalline rods by the floating zone recrystallization method. Samples were 3–5 mm long and had a cross section of $0.2-0.4$ mm^2. The resistivity and Hall-effect data that will be presented here are for **a** and **c** axes. The **c** direction is the highest conductivity direction (along ladders and chains), the **a** direction with intermediate conductivity is perpendicular to **c** in the **a**-**c** ladder plane, while the **b** direction (with the lowest conductivity) is perpendicular to the **a**-**c** plane. For the **c** and **a** axes resistivity measurements, the samples have been cut from a long single crystal along the **c** and **a** axes.

Electrical contacts to the sample (three pairs of Hall contacts and one pair of current contacts on the sides of the crystal) were obtained by using a special DuPont 6838 silver paste. The paste was first applied directly to the surface and heated for 1 h at 450 °C in oxygen flow atmosphere, and then the 30 μm gold wires were pasted to the baked contact areas of the sample.

The measurements were conducted in the temperature range 4.2 K$<T<$300 K. Due to the semiconducting nature of the samples, the electrical resistances varied from ~ 1 Ω to ~ 100 MΩ; depending on the resistance, either ac or dc techniques were used for the measurements. For resistivity measurements two pairs of voltage contacts on each side of the sample were used.

The Hall effect was measured in 5 and 9 T magnetic fields. The magnetic field was always along the **b** direction (**B**$\|$**b** geometry). For all the samples ($0 \leq x \leq 11.5$) the current was **j**$\|$**a**, whereas for $x=0$ and $x=11.5$, Hall data were also taken for current along the **c** direction (this enabled us to check the possible anisotropy in the Hall effect). The latter geometry would have been a preferred choice, but for some samples, on our disposal, it was not eligible (for accurate
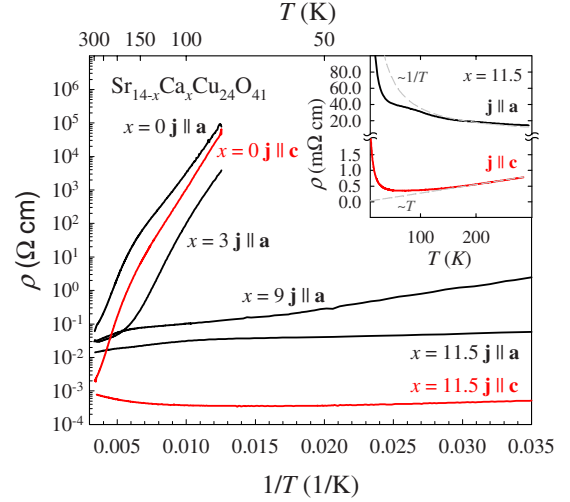

FIG. 1. (Color online) Temperature dependence of the dc resistivity, ρ vs $1/T$ for different $Sr_{14-x}Ca_xCu_{24}O_{41}$ compounds measured along **a** direction **j**$\|$**a** (black lines) and along **c** direction **j**$\|$**c** [red (gray) lines]. Inset: Temperature dependence ρ vs T of the resistivity for $x=11.5$ compound for **j**$\|$**a** and **j**$\|$**c**. Dashed lines present related power laws.

Hall-effect measurements) to measure in that geometry due to unnested voltages greater than 20% (which are an indication of inhomogeneous current flow). To decrease the inhomogeneous current flow a mechanical removing (by using the emery paper) of the surface layer is important and was performed whenever it was possible for our samples.

Particular care was taken to ensure the temperature stabilization. The Hall voltage was measured at fixed temperatures for all three pairs of Hall contacts to test and/or control the homogenous current distribution through the sample and in field sweeps from $-B_{max}$ to $+B_{max}$ in order to eliminate the possible mixing of magnetoresistive components (due to the misalignment of the opposite Hall contacts). Also, two contacts along one side of the sample could be used as a pair of voltage contacts to compensate (at zero field) the Hall signal, eliminating in that way the magnetoresistive component directly from the measured data and thus increasing the accuracy of the Hall signal measurements. As it will be shown later, the Hall resistivity is linear with applied fields up to 9 T. The Hall coefficient R_H is obtained as $R_H=(V_{xy}/IB)t$, where V_{xy} is Hall voltage determined as $[V_{xy}(B)-V_{xy} \times(-B)]/2$, I is the current through the crystal, and t is the sample thickness. The presented R_H values are mean values (obtained for three pairs of Hall contacts) and the error bars are the variance.

III. RESULTS

Figure 1 shows the dependence of the resistivity $\rho(T)$ on inverse of temperature $1/T$, for $Sr_{14-x}Ca_xCu_{24}O_{41}$ in the temperature range 20 K$<T<$300 K, measured on samples with calcium part $x=0$, $x=3$, $x=9$, and $x=11.5$ along **a** direction (**j**$\|$**a**) and **c** direction (**j**$\|$**c**). The detailed resistivity measurements (from 2 to 750 K) on the same samples (except $x=0$, **j**$\|$**c**) were already done previously (for more de-
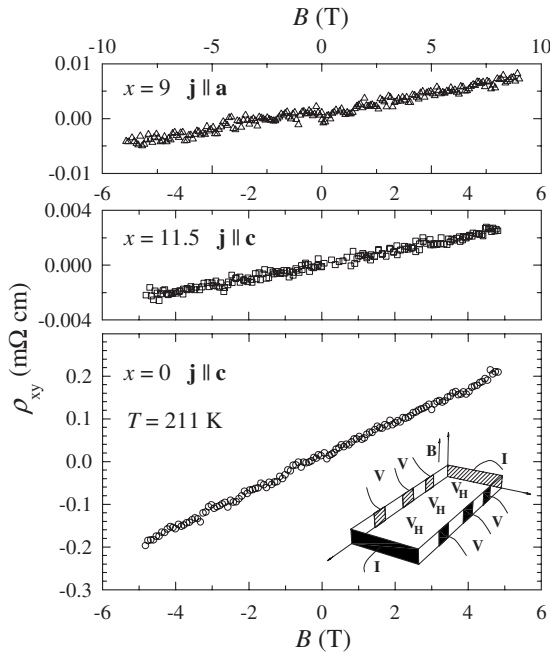
FIG. 2. Magnetic-field dependence of the Hall resistivity ρ_{xy} of $Sr_{14-x}Ca_xCu_{24}O_{41}$ for $x=0$ and 11.5 ($\mathbf{j}\|\mathbf{c}$ and $\mathbf{B}\|\mathbf{b}$ up to 5 T) and for $x=9$ ($\mathbf{j}\|\mathbf{a}$ and $\mathbf{B}\|\mathbf{b}$ up to 9 T); all at $T=211$ K. Also shown is the sample geometry and the arrangement of contacts.

tails see Refs. [2], [18], and [19]). For our measurements the samples were cleaned up, new contacts mounted and resistivity remeasured. The same samples were used for Hall-effect measurements as well. The room-temperature resistivity values for **a** direction range from 70 mΩ cm for $x=0$ to 13 mΩ cm for $x=11.5$, and in **c** direction from 10 mΩ cm to 1 mΩ cm, which is in good agreement with the previously published data.[2,8,18,19] The presented results refer to samples with homogeneous current flow and the same samples were used for Hall-effect measurements as well.

The temperature dependence of resistivity, which is rather different for various x is in good agreement with the previously published data.[2,8,18,19] For $x\leq9$, $\rho_{a,c}(T)$ can be analyzed using a phenomenological law for a semiconductor, $\rho \propto \exp[\Delta/T]$: for $x\leq9$ all the samples are semiconducting already at room temperature (for both **a** and **c** directions). The extracted high-temperature activation energies are $\Delta \sim 1000$ K for $x=0$ sample, $\Delta\sim500$ K for $x=3$, and $\Delta \sim 120$ K for $x=9$ (Refs. [2] and [18]). At lower temperatures, the fact that for $x=0$ the activation energy below about 150 K appears to be lower for $\rho_a(T)$ than for $\rho_c(T)$ is most probably sample dependent since we have used two different samples for these measurements. The $x=11.5$ sample shows a resistivity increase with decreasing temperature for **a** direction and a metallic behavior in **c** direction down to around 80 K and semiconducting at lower temperatures, as already known.[8,18,19] In the temperature region 140 K$<T<300$ K, $\rho_a(T)$ follows almost T^{-1} while $\rho_c(T)$ follows linear T dependence (this different temperature variation is seen the best in the inset of Fig. 1 where the dashed lines present related power laws).

Figure 2 shows the magnetic-field dependence of the Hall resistivity ρ_{xy}, at fixed temperature $T=211$ K, for three
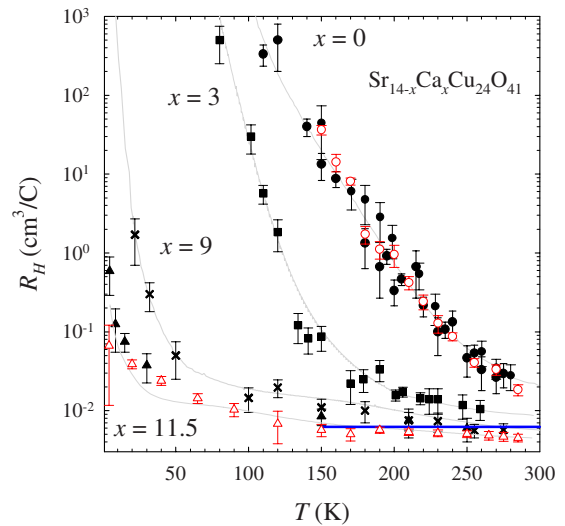

FIG. 3. (Color online) Temperature dependence of the Hall coefficient R_H for different $Sr_{14-x}Ca_xCu_{24}O_{41}$ compounds. Full symbols are for $\mathbf{j}\|\mathbf{a}$ geometry and empty symbols for $\mathbf{j}\|\mathbf{c}$ geometry. The gray lines are scaled temperature dependences of resistivity measured in $\mathbf{j}\|\mathbf{a}$ geometry. The solid straight horizontal blue (gray) line is the calculated value for the Hall coefficient (see text).

samples $Sr_{14-x}Ca_xCu_{24}O_{41}$ $x=9$ ($\mathbf{j}\|\mathbf{a}$), $x=11.5$ ($\mathbf{j}\|\mathbf{c}$), and $x =0$ ($\mathbf{j}\|\mathbf{c}$). Similar ρ_{xy} vs B sweeps at other fixed temperatures show that the Hall resistivity is linear with field up to 9 T in the whole temperature interval investigated and that the sign of the Hall coefficient is positive.

For the $Sr_{14-x}Ca_xCu_{24}O_{41}$ family, results from Hall effect experiments for the $x=12$ compound at applied pressures of 0.3 and 1.0 GPa have been published.[20] Our resistivity results follow those published previously at ambient pressure.[2]

Figure 3 shows the temperature dependence of the Hall coefficient R_H for $Sr_{14-x}Ca_xCu_{24}O_{41}$ in the temperature range 4.2 K$<T<300$ K, measured on samples with calcium part $x=0$ ($\mathbf{j}\|\mathbf{a},\mathbf{B}\|\mathbf{b}$) ($\mathbf{j}\|\mathbf{c},\mathbf{B}\|\mathbf{b}$), $x=3$ ($\mathbf{j}\|\mathbf{a},\mathbf{B}\|\mathbf{b}$), $x=9$ ($\mathbf{j}\|\mathbf{a},\mathbf{B}\|\mathbf{b}$) and $x=11.5$ ($\mathbf{j}\|\mathbf{a},\mathbf{B}\|\mathbf{b}$) ($\mathbf{j}\|\mathbf{c},\mathbf{B}\|\mathbf{b}$). Each Hall coefficient value was determined from one or more magnetic-field sweeps at a fixed temperature.

The scaled temperature dependences of the resistivity for the related samples (shown as gray lines in Fig. 3) indicate that the resistivity and the Hall coefficient follow the same exponential law with the same activation energy. Furthermore, our measurements do not show any anisotropy in the Hall effect: for $x=0$ and $x=11.5$ samples, the temperature dependences of R_H are (within the experimental error) the same for ($\mathbf{j}\|\mathbf{a},\mathbf{B}\|\mathbf{b}$) and ($\mathbf{j}\|\mathbf{c},\mathbf{B}\|\mathbf{b}$) geometry. The measurements were done during cooling and heating; the error bars indicate the changes in R_H due to very small temperature variations during magnetic-field sweeps (this particularly refers to the region where the resistivity changes strongly with temperature).

The solid straight horizontal blue (gray) line in Fig. 3 represents the calculated value of the Hall coefficient obtained assuming that 5 of the 6 self-doped holes per f.u. are localized on the chains and one of them is delocalized on the ladders.[12] In this case the carrier concentration is $\sim10^{21}$ cm^{-3} which yields (by using the simple model) R_H

$=1/ne=6.25\times10^{-3}$ cm^3/C (e is the electronic charge). As shown, the room-temperature Hall coefficient values for all samples—except the $x=0$ one—are close to this calculated value. This issue will be discussed later. Another feature, which will also be discussed later in more detail, is that for the $x=11.5$ compound the temperature variation of the Hall coefficient (for both current directions) follows only the **j**∥**a** resistivity (semiconducting) behavior.

IV. DISCUSSION

A first comprehensive investigation of the anisotropic electrical resistivity of Sr$_{14-x}$Ca$_x$Cu$_{24}$O$_{41}$ single crystals at ambient pressure was performed by Motoyama *et al.*;[8] later a number of groups continued and extended these studies. The most detailed dc electrical transport investigation of Sr$_{14-x}$Ca$_x$Cu$_{24}$O$_{41}$ single crystals (with $x=0$, 3, 6, 8, 9, and 11.5) was performed by Vuletić *et al.*[2] covering a large range of temperature and all three crystallographic directions. Our resistivity results follow these data closely. All the single crystals for **j**∥**c** and **j**∥**a** (except **j**∥**c** for $x=11.5$) exhibit a rapid increase in the resistivity upon cooling, following the activated behavior characteristic for semiconductors. Calcium substitution suppresses the activation energy (from 80 meV for $x=0$ to 9 meV for $x=9$; see Ref. 2 for more details). The value of **a**-axis resistivity (ρ_a) is larger than the **c**-axis resistivity (ρ_c) by 1 to 2 orders of magnitude and for $0\leq x<11.5$ shows approximately the same activated behavior. As a consequence, the anisotropy ratio (ρ_a/ρ_c) neither depends strongly on T at high temperatures nor varies basically with Ca content.

As it was already shown,[8] the dc resistivity for $x=11.5$ exhibits a different behavior than all other $0\leq x<11.5$ compounds: although at low temperatures, below ≈50 K, the resistivity ρ_c increases (as it does for **j**∥**a** direction, indicating a carrier localization), a metallic behavior is seen above 80 K. In other words, the T dependence of ρ_a (which is anomalous in the sense that $d\rho_a/dT<0$, i.e., semiconducting, in the temperature range where $d\rho_c/dT>0$, i.e., metallic) indicates a noncoherent transport along the **a** axis (along the rungs of the ladders). Moreover, an insulator-to-superconductor transition was observed at ∼4.0 GPa, accompanied by incoherent to coherent crossover of the transverse (interladder, **a** axis) charge transport; i.e., ρ_c and ρ_a have shown quite similar metallic temperature dependences, which indicates that both are subject to the same scattering mechanism.[21] The application of pressure therefore triggers a dimensional crossover in the charge dynamics from one to two, and the superconductivity in this ladder compound might be a phenomenon in a two-dimensional (2D) anisotropic electronic system. Such findings indicate that, at ambient pressure, charge dynamics is essentially one dimensional (1D) and carriers are confined within each ladder.

The phenomenon of interlayer or interchain decoherence in anisotropic metals is still poorly understood. In strictly 1D systems all electronic states are known to be localized at $T=0$ in the presence of weak disorder, whereas in real materials with finite interchain coupling $t_\perp$, the situation is different. A considerable theoretical work has been devoted to this subject.[4,22] Recently, in accord with Prigodin and Firsov's[23] argumentation that impurity scattering rates $\hbar/\tau_0>t_\perp$ render the system effectively 1D and therefore susceptible to localization at low T, the influence of introduced disorder on anisotropic resistivity of PrBa$_2$Cu$_4$O$_8$ was analyzed and interpreted as a consequence of localization effects that are observed for extremely small amounts of disorder.[24] In other words, once the intrachain scattering rate surpasses the interchain hopping rate, the coherent interchain tunneling is suppressed, the system is rendered effectively 1D, and localization sets in. We believe that this finding shows qualitative agreement with our $\rho(T)$ data for $x=11.5$ (the metallic-like behavior in one direction only). In Sr$_{14-x}$Ca$_x$Cu$_{24}$O$_{41}$ an incommensurability between the chains and ladders creates distortions, which lead to additional modulations of the crystallographic positions that are intrinsic sources of disorder. Moreover, there is an additional disorder introduced by Ca substitution.[2] Accordingly, the difference in the $\rho_c(T)$ and $\rho_a(T)$ behavior of $x=11.5$ compound may be attributed to intrinsic disorder while the appearance of a metallic behavior for $\rho_a(T)$ under pressure[21] indicates that the interladder coupling starts to prevail over one-dimensional (1D) effects, which dominate the charge transport at ambient pressure.

Our results give a positive, holelike, Hall coefficient which is temperature dependent for all Sr$_{14-x}$Ca$_x$Cu$_{24}$O$_{41}$ samples. For two concentrations ($x=0$ and $x=11.5$) the measurements were performed in both geometries **j**∥**c**, **B**∥**b** and **j**∥**a**, **B**∥**b** giving similar values (cf. Fig. 3), thus indicating no anisotropy in $R_H(T)$. According to Onsager's[25] reciprocal relation for **B**∥**b**, R_H measured in **j**∥**a** and **j**∥**c** geometry is the same unless the time-reversal symmetry is broken. Since we observe that the temperature dependence of R_H measured in both geometries is approximately the same (the observed small differences in absolute Hall coefficient values are within experimental uncertainties) we take that Onsager's relation is satisfied for Sr$_{14-x}$Ca$_x$Cu$_{24}$O$_{41}$ and we comprehend both geometries as a good choice to determine $R_H(T)$.

Turning now to the concentration variation of the Hall data, we first analyze the $x<11.5$ results. For $0\leq x<11.5$ both $R_H(T)$ and $\rho(T)$ follow the same temperature dependences. Their behavior is comparable to a conventional p-type semiconductor, where at high enough temperature all doped holes are activated and the effective number of carriers $n_{eff}\sim 1/eR_H$ saturates.[26] The Hall coefficient increases with decreasing temperature; i.e., $R_H(T)\propto\exp\{\Delta/T\}$ is thermally activated and the activation energy Δ for $x<11.5$ agrees well with that obtained from the resistivity data. For $x=0$ (and possibly $x=3$) n_{eff} is not fully saturated at 300 K (because $\Delta\gg T$), and the actual hole number is higher.

From the measured Hall coefficient R_H values for different Ca substitutions (Fig. 4) we can calculate the effective number of carriers $n_{eff}=V/(4eR_H)$ per f.u. at room temperature (V is the volume of the unit cell, e is the electronic charge, and the factor 4 in the denominator describes that the unit cell contains 4 f.u.; the changes in the unit cell volume with Ca content have been taken into account[6,7,9]). For $x=11.5$ we consider that $R_H(T)$ values at temperatures that approach room temperature do not change significantly (and we calculate n_{eff} in an equivalent way as for $x<11.5$); the related temperature dependence will be discussed more in the
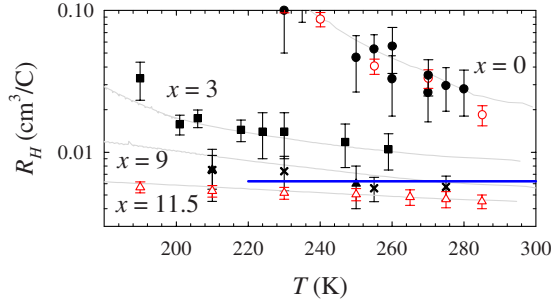
FIG. 4. (Color online) High-temperature R_H vs T, presented in more detail in order to emphasize the values around 300 K.

last part of this section. The n_{eff} values are displayed in Fig. 5. The same figure also shows the number of holes per f.u. (n) in $Sr_{14-x}Ca_xCu_{24}O_{41}$ ladders for $0 \le x \le 12$ obtained by different experimental techniques.[11,12,16,17]

Comparing our n_{eff} values with n obtained from other experiments,[11,12,16,17] we find good agreement with NEXAFS and NMR results,[12,16] while optical[11] and resonant soft x-ray scattering[17] data give much higher values, and at this point we cannot clarify the origin of this discrepancy. Our measurements yield for the $n_{eff}(x=11.5) - n_{eff}(x=0)$ a value which agrees with Refs. 12 and 16 bearing in mind the inaccuracy in the determination of $n_{eff}(x=0)$. We believe that our result describes well the fact that a minor change in number of carriers on the ladders is responsible for a pronounced change in resistivity with Ca doping. Here we compare our results of R_H for $x=11.5$, especially around room temperature, where $R_H \approx 4.5 \times 10^{-3}$ cm^{-3}/C (that gives $n_{eff} \approx 1.3$ per f.u. in the ladder) with the published data on temperature dependence of Hall coefficient for $x=12$ at pressures of 0.3 and 1.0 GPa (Ref. 20), which give around room temperature $R_H \approx 2 \times 10^{-3}$ cm^{-3}/C. The considerable reduction in R_H around room temperature under pressure confirms the NMR data[16] where it was suggested that the important role of high pressure for reaching conditions for the stabilization of superconductivity in $Sr_2Ca_{12}Cu_{24}O_{41}$ is an increase in the hole

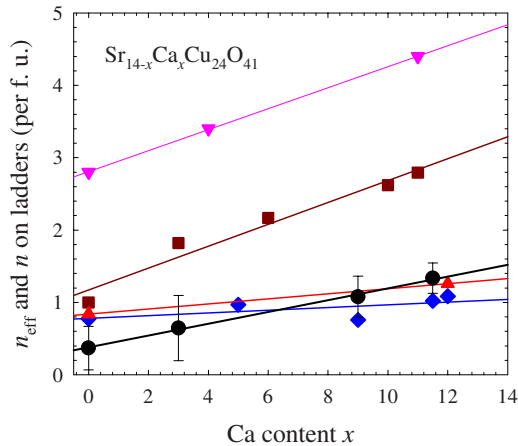FIG. 5. (Color online) The effective number of carriers $n_{eff} = V/(4eR_H)$ (● our data) and the number of holes n per f.u. in the ladder vs calcium content x in $Sr_{14-x}Ca_xCu_{24}O_{41}$. [Data taken from ■ Osafune *et al.* (Ref. 11), ◆ Nücker *et al.* (Ref. 12), ▲ Piskunov *et al.* (Ref. 16), and ▼ Rusydi *et al.* (Ref. 17).]
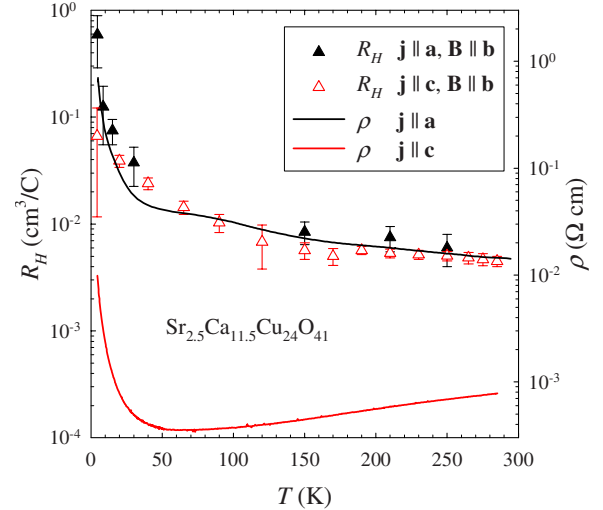

FIG. 6. (Color online) Temperature dependence of the Hall coefficient R_H and resistivity ρ_c and ρ_a for the $x=11.5$ compound of $Sr_{14-x}Ca_xCu_{24}O_{41}$. Full symbols are R_H for $\mathbf{j} \| \mathbf{a}$ geometry and empty symbols for $\mathbf{j} \| \mathbf{c}$ geometry. Red (gray) line: ρ_c, black line: ρ_a.

density in the ladder layers. Note finally that it was also suggested[16] that the hole distribution is temperature dependent and that the back-transfer of holes from the ladders into the chains takes place gradually with decreasing temperature, but we cannot speculate about that from Hall-effect data. To summarize this part of the discussion, we can point out that the effective number of carriers n_{eff} corresponds to the number of holes per f.u. in the ladder obtained by other important experimental techniques. Assuming that Cu-O chains do not contribute to the Hall effect (the holes on the chains are localized[2]) we can conclude that n_{eff} denote the holes in the ladders that participate in dc transport.

Our results for $x=11.5$ are quite different. Figure 6 shows in more detail the temperature dependence of $\rho_c(T)$, $\rho_a(T)$, and the Hall coefficient $R_H(T)$ in both $\mathbf{j} \| \mathbf{a}$, $\mathbf{B} \| \mathbf{b}$ and $\mathbf{j} \| \mathbf{c}$, $\mathbf{B} \| \mathbf{b}$ geometry (as already pointed out and presented in Fig. 6, the Hall coefficient is isotropic). Here we should mention that the published data on pressure dependence of Hall coefficient for $x=12$ at pressures of 0.3 and 1.0 GPa have shown different temperature dependences for $R_H(T)$ ($\mathbf{j} \| \mathbf{c}$ $\mathbf{B} \| \mathbf{b}$) and $\rho_c(T)$.[20] Our results show that although the $R_H(T)$ values do not differ for two different current directions, the temperature variation in $R_H(T)$ follows that of $\rho_a(T)$. The different temperature variation in $R_H(T)$ and $\rho_c(T)$ is particularly evident above 140 K: while $\rho_c(T)$ increases linearly with temperature, the Hall coefficient is proportional to $1/T$.

Such a behavior is typical for high-temperature copper-oxide superconductors, albeit in a broad temperature interval, which metallic state is characterized by unusual and distinct temperature dependences in the transport properties[3,4] that deviate from the conventional Fermi-liquid behaviors. Optimally doped cuprates are characterized by a linear-T resistivity that survives for all $T > T_c$, while the in-plane Hall coefficient varies approximately as $1/T$ over a wide temperature range.[27,28] The R_H of the hole-doped high-T_c cuprates varies markedly with both the number of holes doped onto the copper-oxide planes and temperature. The inverse Hall angle
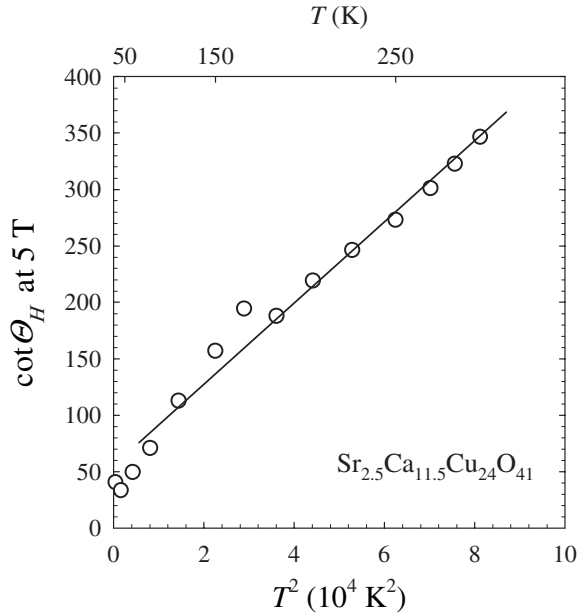
FIG. 7. T^2 dependence of $\cot \theta_H$ (at 5 T) for $x=11.5$ in $Sr_{14-x}Ca_xCu_{24}O_{41}$.

$\cot \theta_H = \rho_{ab}/R_H B$ shows a quadratic T dependence over a remarkably broad temperature range and holds for a wide range of doping in most cuprates[4,29] (ρ_{ab} denotes in-plane resistivity). This unconventional behavior has led theorists to develop a number of models with different approaches, such as two-lifetime picture of Anderson,[30] marginal Fermi-liquid phenomenology,[31] and models based on fermionic quasiparticles that invoke specific (anisotropic) scattering mechanisms within the basal plane.[27,32–36] Currently, the overall experimental situation does appear to support models in which anisotropic linear-T scattering, in conjunction with the Fermi surface curvature and band anisotropy, is primarily responsible for the T dependence of ρ_{ab} and $R_H(T)$. However, the origin of the anisotropic scattering is not known at present,[4] and new interpretations of the normal state transport properties of high T_c are expected.

Figure 7 shows $\cot \theta_H = \rho_c/R_H B$ (at 5 T) vs T^2 for $x=11.5$ compound, and it is clearly perceived that for $T > 140$ K the inverse Hall angle follows T^2 dependence up to room temperature. Since the unusual temperature dependences of ρ_{ab} and $R_H(T)$ of high-temperature copper-oxide superconductors are frequently ascribed to the intrinsic property of the CuO_2 planes, it is quite interesting that similar behavior is now found for highly anisotropic Cu_2O_3 ladder plane. The **a**-**b** plane in high T_c is almost isotropic, with metallic-like resistivities for both perpendicular directions. On the other hand, for $Sr_{14-x}Ca_xCu_{24}O_{41}$ and $x=11.5$ the anisotropy ratio ρ_a/ρ_c is around 13 at room temperature and becomes enhanced at lower temperatures reaching about 55

at 140 K (due to metallic-like $\rho_c(T)$ and non-metallic-like $\rho_a(T)$ variations). This leads to the interesting conclusion: the well-known T^2 dependence of the inverse Hall angle, which seems to be largely doping independent in cuprates,[37,38] is not changed by the increased anisotropy in the ladder plane. Further investigations comprising pressure dependence of $\rho_c(T)$, $\rho_a(T)$, and $R_H(T)$ for different pressures (up to the pressures when superconductivity occurs) and different x may give more information about the normal state properties of $Sr_{14-x}Ca_xCu_{24}O_{41}$ and could be an important step toward a correct microscopic theory of cuprate superconductivity.

V. CONCLUSION

In summary, we have reported measurements of the Hall coefficient $R_H(T)$ at ambient pressure of the quasi-one-dimensional cuprate $Sr_{14-x}Ca_xCu_{24}O_{41}$ for $0 \leq x \leq 11.5$. It is known that isovalent Ca substitution does not change the total hole count, but causes additional transfer of holes from the chains (where they are localized) into the ladders (where they are rather mobile), but as far as the amount of transferred holes is concerned, the experiments which have been performed up to now have given contradictory results.

Our findings give a positive, holelike, Hall coefficient which is temperature dependent for all samples. For $x < 11.5$ the Hall coefficient is activated, and the activation energy agrees well with that obtained from the resistivity data. The observed behavior is that of a conventional p-type semiconductor. For $x=11.5$ $\rho_c(T)$ and $R_H(T)$ follow different temperature dependences: above 140 K $\rho_c(T)$ increases linearly with temperature, while the Hall coefficient is inversely proportional to T, giving an overall T^2 dependence of the inverse Hall angle $\cot \theta_H$ for 140 K $< T <$ 300 K. Such behavior, which is well known and typical for high-temperature copper-oxide superconductors, seems independent of the pronounced anisotropy in the Cu_2O_3 ladder plane.

A comparison of our estimate for the effective number of carriers $n_{eff} \sim 1/R_H$ for $Sr_{14-x}Ca_xCu_{24}O_{41}$ ($0 \leq x \leq 11.5$) at 300 K with the numbers of holes in ladders (obtained by different experimental techniques) shows good agreement with NEXAFS and NMR results and indicates that n_{eff} corresponds to the holes in the ladders that participate in dc transport. The difference $n_{eff}(x=11.5) - n_{eff}(x=0) = 0.96$ (this value could be even lower due to, probably underestimated, n_{eff} for $x=0$) leads us to conclude that a minor change in number of carriers on the ladders is responsible for a pronounced change in resistivity with Ca substitution.

*etafra@phy.hr

[1] E. Dagotto, Rep. Prog. Phys. **62**, 1525 (1999).

[2] T. Vuletić, B. Korin-Hamzić, T. Ivek, S. Tomić, B. Gorshunov, M. Dressel, and J. Akimitsu, Phys. Rep. **428**, 169 (2006).

[3] E. Dagotto, Rev. Mod. Phys. **66**, 763 (1994).

[4] N. E. Hussey, J. Phys.: Condens. Matter **20**, 123201 (2008).

[5] M. Uehara, T. Nagata, J. Akimitsu, H. Takahashi, N. Môri, and K. Kinoshita, J. Phys. Soc. Jpn. **65**, 2764 (1996).

[6] T. Siegrist, L. F. Schneemeyer, S. A. Sunshine, J. V. Waszczak, and R. S. Roth, Mater. Res. Bull. **23**, 1429 (1988).

[7] E. M. McCarron III, M. A. Subramanian, J. C. Calabrese, and R. L. Harlow, Mater. Res. Bull. **23**, 1355 (1988).

[8] N. Motoyama, T. Osafune, T. Kakeshita, H. Eisaki, and S. Uchida, Phys. Rev. B **55**, R3386 (1997).

[9] M. Isobe, T. Ohta, M. Onoda, F. Izumi, S. Nakano, J. Q. Li, Y. Matsui, E. Takayama-Muromachi, T. Matsumoto, and H. Hayakawa, Phys. Rev. B **57**, 613 (1998).

[10] Y. Mizuno, T. Tohyama, and S. Maekawa, J. Phys. Soc. Jpn. **66**, 937 (1997).

[11] T. Osafune, N. Motoyama, H. Eisaki, and S. Uchida, Phys. Rev. Lett. **78**, 1980 (1997).

[12] N. Nücker, M. Merz, C. A. Kuntscher, S. Gerhold, S. Schuppler, R. Neudert, M. S. Golden, J. Fink, D. Schild, S. Stadler, V. Chakarian, J. Freeland, Y. U. Idzerda, K. Conder, M. Uehara, T. Nagata, J. Goto, J. Akimitsu, N. Motoyama, H. Eisaki, S. Uchida, U. Ammerahl, and A. Revcolevschi, Phys. Rev. B **62**, 14384 (2000).

[13] Y. Gotoh, I. Yamaguchi, Y. Takahashi, J. Akimoto, M. Goto, M. Onoda, H. Fujino, T. Nagata, and J. Akimitsu, Phys. Rev. B **68**, 224108 (2003).

[14] K. Magishi, S. Matsumoto, Y. Kitaoka, K. Ishida, K. Asayama, M. Uehara, T. Nagata, and J. Akimitsu, Phys. Rev. B **57**, 11533 (1998).

[15] K. R. Thurber, K. M. Shen, A. W. Hunt, T. Imai, and F. C. Chou, Phys. Rev. B **67**, 094512 (2003).

[16] Y. Piskunov, D. Jérome, P. Auban-Senzier, P. Wzietek, and A. Yakubovsky, Phys. Rev. B **72**, 064512 (2005).

[17] A. Rusydi, M. Berciu, P. Abbamonte, S. Smadici, H. Eisaki, Y. Fujimaki, S. Uchida, M. Rübhausen, and G. A. Sawatzky, Phys. Rev. B **75**, 104510 (2007).

[18] T. Vuletić, B. Korin-Hamzić, S. Tomić, B. Gorshunov, P. Haas, T. Rõõm, M. Dressel, J. Akimitsu, T. Sasaki, and T. Nagata, Phys. Rev. Lett. **90**, 257002 (2003).

[19] T. Vuletić, T. Ivek, B. Korin-Hamzić, S. Tomić, B. Gorshunov, P. Haas, M. Dressel, J. Akimitsu, T. Sasaki, and T. Nagata, Phys. Rev. B **71**, 012508 (2005).

[20] T. Nakanishi *et al.*, J. Phys. Soc. Jpn. **67**, 2408 (1998).

[21] T. Nagata, M. Uehara, J. Goto, J. Akimitsu, N. Motoyama, H. Eisaki, S. Uchida, H. Takahashi, T. Nakanishi, and N. Môri, Phys. Rev. Lett. **81**, 1090 (1998).

[22] T. Ishiguro, K. Yamaji, and G. Saito, *Organic Superconductors*, 2nd ed. (Springer, Berlin, 1998).

[23] V. N. Prigodin and Y. A. Firsov, Pis'ma Zh. Eksp. Teor. Fiz. **38**, 241 (1983) [JETP Lett. **38**, 284 (1983)].

[24] A. Enayati-Rad, A. Narduzzo, F. Rullier-Albenque, S. Horii, and N. E. Hussey, Phys. Rev. Lett. **99**, 136402 (2007).

[25] L. Onsager, Phys. Rev. **38**, 2265 (1931).

[26] R. A. Smith, *Semiconductors* (Cambridge University Press, Cambridge, England, 1968).

[27] A. Carrington, A. P. Mackenzie, C. T. Lin, and J. R. Cooper, Phys. Rev. Lett. **69**, 2855 (1992).

[28] H. Y. Hwang, B. Batlogg, H. Takagi, H. L. Kao, J. Kwo, R. J. Cava, J. J. Krajewski, and W. F. Peck, Phys. Rev. Lett. **72**, 2636 (1994).

[29] S. Ono, S. Komiya, and Y. Ando, Phys. Rev. B **75**, 024515 (2007).

[30] P. W. Anderson, Phys. Rev. Lett. **67**, 2092 (1991).

[31] C. M. Varma, P. B. Littlewood, S. Schmitt-Rink, E. Abrahams, and A. E. Ruckenstein, Phys. Rev. Lett. **63**, 1996 (1989).

[32] N. E. Hussey, Eur. Phys. J. B **31**, 495 (2003).

[33] C. Castellani, C. Di Castro, and M. Grilli, Phys. Rev. Lett. **75**, 4650 (1995).

[34] L. B. Ioffe and A. J. Millis, Phys. Rev. B **58**, 11631 (1998).

[35] A. T. Zheleznyak, V. M. Yakovenko, H. D. Drew, and I. I. Mazin, Phys. Rev. B **57**, 3089 (1998).

[36] M. Abdel-Jawad, M. P. Kennett, L. Balicas, A. Carrington, A. P. Mackenzie, R. H. McKenzie, and N. E. Hussey, Nat. Phys. **2**, 821 (2006).

[37] I. Kokanović, J. R. Cooper, S. H. Naqib, R. S. Islam, and R. A. Chakalov, Phys. Rev. B **73**, 184509 (2006).

[38] Y. Ando, Y. Kurita, S. Komiya, S. Ono, and K. Segawa, Phys. Rev. Lett. **92**, 197001 (2004).